

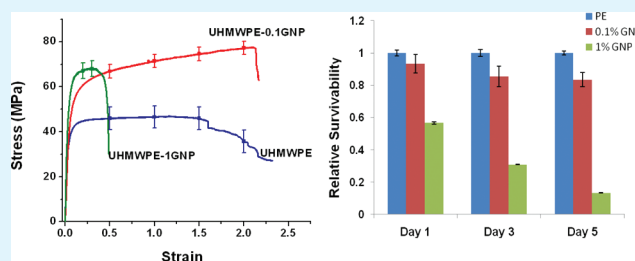
Graphene Nanoplatelet-Induced Strengthening of UltraHigh Molecular Weight Polyethylene and Biocompatibility In vitro

Debrupa Lahiri,[†] Rupak Dua,[‡] Cheng Zhang,[†] Ignacio de Socarraz-Nova,[†] Ashwin Bhat,[†] Sharan Ramaswamy,[‡] and Arvind Agarwal^{*,†}

[†]Plasma Forming Laboratory, Mechanical and Materials Engineering [‡]Biomedical Engineering Florida International University, Miami, Florida 33174, United States

ABSTRACT: Graphene nanoplatelets (GNPs) are added as reinforcement to ultrahigh molecular weight polyethylene (UHMWPE) with an intended application for orthopedic implants. Electrostatic spraying is established as a potential fabrication method for synthesizing large-scale UHMWPE-GNP composite films. At a low concentration of 0.1 wt % GNP, the composite film shows highest improvement in fracture toughness (54%) and tensile strength (71%) as compared to UHMWPE. Increased GNP content of 1 wt % leads to improvement in elastic modulus and yield strength but fracture toughness and tensile strength are reduced significantly at higher GNP content. The strengthening mechanisms of the UHMWPE-GNP system are highly influenced by the GNP concentration, which dictates its degree of dispersion and extent of polymer wrapping. The fraction of GNPs oriented along the tensile axis influences the elastic deformation, whereas the wrapping of polymer and GNP-polymer interfacial strength determines the deformation behavior in the plastic regime. The cytotoxicity of GNP to osteoblast is dependent on its concentration and is also influenced by agglomeration of particles. Lowering the concentration of GNPs in UHMWPE improves the biocompatibility of the composite surface to bone cells. The survivability of osteoblasts deteriorates up to 86% on 1 wt % GNP containing surface, whereas much smaller (6–16%) reduction is observed for 0.1 wt % GNP over 5 days of incubation.

KEYWORDS: graphene nanoplatelet, ultrahigh molecular weight polyethylene, composite, strengthening, osteoblast, cytotoxicity



1. INTRODUCTION

Graphene has been widely researched in recent times, because of its outstanding electrical, chemical, and mechanical properties. It is of great interest as reinforcement to structural composites, due to its excellent mechanical properties, viz., 0.5–1 TPa elastic modulus¹ and 130 GPa tensile strength.² It has been successfully used as reinforcement for several polymer matrices.^{2–17} Apart from electrical and thermal properties, polymer–graphene composites also possess improved elastic modulus, hardness, toughness and fatigue strength.^{2–10,16,17} The main advantages of graphene as reinforcement to structural composites are its excellent in-plane strength and very high surface area, which leads to enhanced load-transfer sites between the matrix and reinforcement.

Ultrahigh molecular weight polyethylene (UHMWPE) is a clinical grade polymer used as a linear in modular acetabular cup designs of the hip implant. The UHMWPE linear prevents metal–metal abrasion between the femoral head and the metallic shell which can result in the generation of cytotoxic metallic wear debris. UHMWPE is also used for similar purposes in knee and other orthopedic implants. However, the primary limitation of UHMWPE is its inherent low strength leading to severe wear and failure of the linear. This leads to premature replacement of implants. Wear debris causes stimulation of inflammatory reactions resulting in osteoly-

sis.^{18,19} Moreover, low yield stress of UHMWPE can lead to permanent deformation and failure at high contact stress.¹⁸ Thus, it is important to improve the mechanical performance of UHMWPE, which can be achieved by using suitable second phase reinforcement; for example, hydroxyapatite (HA) has been used in this manner.^{20,21} Hydroxyapatite has the added advantage of osteoinductive capabilities, however, these studies have used a very high content of reinforcement, as much as 50 wt %, to achieve 100% improvement in the elastic modulus. Addition of HA in UHMWPE decreases the yield strength by 34% and strain by 57% and ultimately, reduction in toughness of the composite, which has a negative effect on the wear resistance.^{20,21}

Carbon nanotubes (CNTs), another high strength allotrope of carbon, have also been investigated for the same purpose.^{22–25} Addition of 1 wt.% CNT in solution casted UHMWPE films show 38% increase in elastic modulus and 49% in yield strength.²⁴ Increased CNT content to 5 wt.% in electrostatically sprayed UHMWPE film showed an 82% increase in elastic modulus, though with a 13% decrease in the fracture strength.²⁵ On the other hand, screw extruded

Received: February 11, 2012

Accepted: March 23, 2012

Published: March 23, 2012

UHMWPE-5 wt % CNT fibers showed a 44% increase in fracture energy, though minimal increase in tensile strength and elastic modulus.²³ Higher CNT content leads to its agglomeration in the composite. Thus, CNTs have not been utilized to their fullest strengthening potential.^{22–25} In the present study, graphene nanoplatelets (GNPs) are evaluated as a potential reinforcement for UHMWPE. The advantages of using GNPs over CNTs in UHMWPE composite could be summarized as follows:

(i) GNPs are easier to disperse uniformly than CNT and would lead to more homogeneous reinforcement phase dispersion in UHMWPE-GNP composite

(ii) Greater surface area of GNPs platelets will create more interfaces and improved bonding, resulting in effective load transfer and increased strength. A higher aspect ratio of CNTs would need a higher concentration than graphene to form a percolated network in composite.^{3–6} A lower amount of the second phase is always better/healthier for biomaterials.

(iii) A 2D graphene layer could provide a higher degree of lubrication during contact-frictional movement of femoral head in acetabular cup, resulting in lesser wear and debris generation.

Although graphene reinforcement in UHMWPE has a lot of potential, only one study has been conducted very recently²⁶ on this material system. But the toughness of UHMWPE pellet, fabricated by extrusion and hot pressing, decreased with 0.5 wt % GNP addition. The reason for such negative effect is reported to be poor distribution of filler phase in matrix. The aim of the present study is to evaluate the potential of GNP reinforcement in UHMWPE, in terms of strengthening and biocompatibility for orthopedic applications. The role of electrostatic spraying as an easy and fast processing route for synthesizing UHMWPE-GNP composite films is also emphasized. Mechanical properties (elastic modulus, tensile strength, and toughness) of the composite film are evaluated through tensile testing. In-vitro biocompatibility of GNP and UHMWPE-GNP composite is assessed with osteoblasts. Biocompatibility of graphene is not in universal agreement thus far. Few studies have shown the cytotoxicity of graphene is dose-dependent and caused by oxidative stress generated in contact with graphene.^{27–29} On the other hand, reports are also available on accelerated bone-cell growth due to selective attachment of growth factors on graphene sheets.^{30–33} This study adds to the continuing scientific discussion on the biocompatibility of graphene, which is still poorly understood.

2. MATERIAL AND METHODS

2.1. Composite Powder Preparation. Graphene nanoplatelets (xGNP-M-5) with ~6–8 nm thickness, 120–150 m²/g surface area and average particle diameters of 5 μm were obtained from XG Sciences, Inc. (Lansing, MI, USA). These platelets were prepared by the exfoliation of graphite. The density of GNP platelets measured through helium pycnometry was 1.8 g/cm³. The UHMWPE powder with density of 0.95 g/cm³ and particle diameter in the range of 20–30 μm was procured from Mitsui Chemical America, Inc. (New York, USA). SEM image of as-received GNP in Figure 1a reveals flaky morphology with cleavage features very characteristic of the exfoliated structure. UHMWPE powders consist of round particles (Figure 1b,c).

GNPs were ultrasonicated for 10 min in acetone for the uniform dispersion. Subsequently, UHMWPE was added and ultrasonicated for another 20 min to obtain a suspension of uniform color indicating homogeneous dispersion. The composite powder was allowed to settle and the excess dispersant was drained. The powder was kept in the oven at 60 °C until it was fully dried. The compositions chosen for this study were UHMWPE, UHMWPE-0.1 wt % GNP and UHMWPE-1 wt % GNP, which would be referred in this study as UHMWPE,

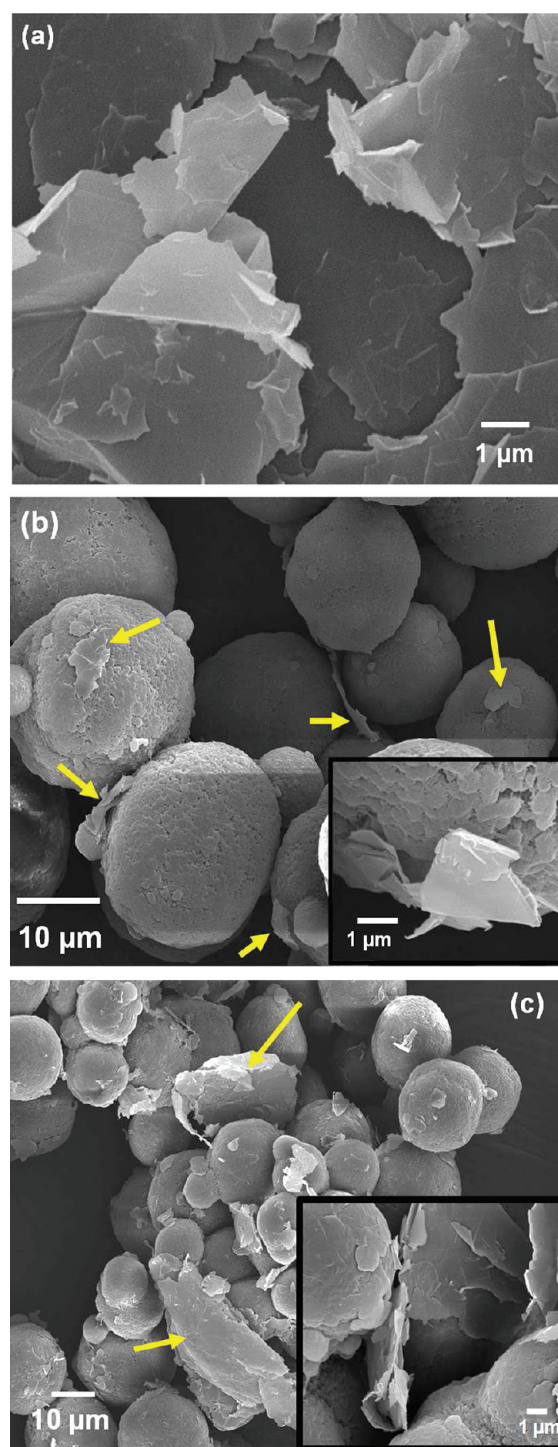


Figure 1. SEM images of (a) exfoliated GNPs with flaky structure; (b) UHMWPE-0.1GNP composite powder showing uniform distribution of GNP and attachment of GNP on polyethylene powder particle surface as inset; (c) UHMWPE-1GNP powder revealing large clusters of GNPs, which remains nonadherent to powder particle surfaces. The arrows in the images indicate GNPs.

UHMWPE-0.1GNP and UHMWPE-1GNP, respectively. The weight fraction of reinforcement phase was kept low in this study, considering very high surface area of GNPs, which has resulted in an impressive improvement of mechanical properties in other polymers.³

2.2. Composite Film Preparation. Electrostatic powder coating system (Craftsman) was used for preparing UHMWPE and UHMWPE-GNP composite films. Electrostatic spraying is an easy

process for preparing uniform powder coating on metallic or electrically conductive surfaces.²⁵ This is a rapid fabrication process of powder coatings with minimal overspray loss, which is followed by the curing treatment to prepare a macro-scale uniform coating. In the present study, three compositions of powders were electrostatically deposited on Teflon coated, nonstick substrates for 3 min. The sprayed substrates were then cured in an oven at 120 °C for 1 h. After ambient cooling, the film was peeled off the substrate. The free-standing film was of circular shape with ~200 mm diameter and ~300 μm thickness.

2.3. Evaluation of Mechanical Properties. Mechanical properties of the UHMWPE based films were evaluated by tensile testing. Tensile samples were 30 mm long, 5 mm wide, and 300 μm thick with a gauge length of 5 mm. These samples were cut from the large composite films synthesized by electrostatic spraying. Tensile sample preparation and tests were carried out in accordance with ASTM-D3039M-08. Tests were carried out using a mechanical testing device (Electroforce 3200 test instrument, Bose Corporation, Eden Prairie, MN) in uniaxial tensile mode using a 10 N load cell and a maximum crosshead movement of 12 mm. The tests were carried out at a crosshead speed of 0.03 mm/s. Extensometer was not used for strain measurement, as the tensile samples were thin and very lightweight. Three samples from each composition have been tested for calculating elastic modulus, tensile strength and toughness. The yield strength is defined at the point of stress–strain curve, where it deviates from the straight line with a single slope.

Scanning electron micrographs of powders, films and fracture surface of tensile specimen were obtained using JEOL JSM-6330 FE-SEM with 5 kV operating voltage and a working distance of 38–39 mm.

2.4. Biocompatibility Evaluation for GNP and UHMWPE-GNP Composite Films. Osteoblasts, the bone forming cells, were chosen for in vitro biocompatibility evaluation. The cytotoxicity of GNP was assessed by culturing osteoblasts in medium with different concentrations of GNP and assessing the cell morphology and viability.

2.4.1. Morphological Observations of Osteoblasts in Graphene Environment. Osteoblasts (ATCC, Manassas, VA) were seeded on 24 well plates using a cell density of 10⁵ cells/ml in Dulbecco's modified eagle medium, (DMEM, Invitrogen, Grand Island, NY) supplemented with 10% fetal bovine serum, (FBS, ATCC, Manassas, VA), 1% Penstrep (ATCC, Manassas, VA) and 0.3 mg/mL of an aminoglycoside antibiotic (Sigma, St Louis, MO). Cells were incubated for 24 h in a humidified environment at 5%CO₂. Following this, the media was removed from the well plates and rinsed several times with phosphate buffer solution (PBS, Fisher Scientific, Pittsburgh, PA). Graphene solutions were subsequently prepared in osteoblast growth media with varying graphene concentrations (μg/mL): 0.1, 0.5, 1, 2.5, 5, 10, and 100. DMEM media in the well plates were replaced with the graphene solution with each concentration covering two wells of the plate. After 5 days, images were taken using an inverted optical microscope (Model IN200A-5M, Amscope, Chino, CA).

2.4.2. Osteoblast Viability on PE–Graphene Film Substrates. Osteoblasts were seeded on to UHMWPE, UHMWPE-0.1GNP and UHMWPE-1GNP films (*N* = 4 specimens/group) with a cell density of 10⁵ cells/ml. Samples were stored in a standard cell culture incubator (humidified environment at 5% CO₂) and subsequently, sulforhodamine B (SRB) assays were performed at day 1, day 3, and day 5 following incubation, to assess cell viability. The SRB assay is based on colorimetric measurement of viable cellular protein. In brief, the cells were first affixed onto the UHMWPE and UHMWPE-GNP films using trichloroacetic acid. Next, the cells were stained using SRB dye that was provided by the assay kit (TOX6, Sigma). Finally, unbound dye was removed using 1% acetic acid. The SRB dye bounded to the cellular protein was extracted using 10 mM Trizma base and absorbance was measured (565 nm wavelength) using a microplate reader (Synergy HT, Biotek Instruments, Inc., Winooski, Vermont). Cellular viability was reported based on “Relative Survival” which was determined from the absorbance values measured. Results were normalized such that the average absorbance of the control was

equal to one. Specifically, the background absorbance was initially subtracted from each of the individual absorbance vales. Next, normalization was performed by dividing each of the absorbances (average and standard deviation values) by the average absorbances of the corresponding control group of cells.

3. RESULTS AND DISCUSSION

3.1. Morphology of the Composite Powders and Films. Images b and c in Figure 1 present the micrographs of UHMWPE-0.1GNP and UHMWPE-1GNP powders respectively. At lower content (0.1 wt %), GNPs disperse uniformly with UHMWPE powder particles. GNPs are attached on the polymer surface (inset, Figure 1b), which could be due to the weak noncovalent (van der Waal's or π – π) attraction between the two species through carbon atoms. On the other hand, 1 wt % addition causes agglomeration of GNP. As a result, large clusters of GNPs are found separated from polymer particles in UHMWPE-1GNP powder (Figure 1c).

Figure 2 presents digital image of macro-size rectangular pieces cut from the circular films of UHMWPE, UHMWPE-

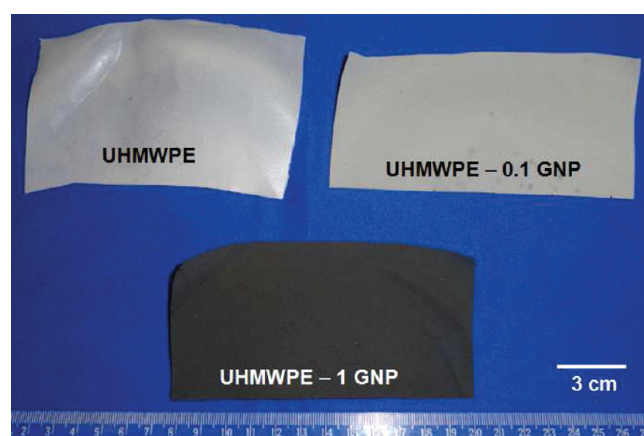


Figure 2. Digital image of the rectangular portions of UHMWPE and UHMWPE composite films cut from the round films.

0.1GNP and UHMWPE-1GNP. The uniform color of the films indicates their uniform thickness. Defect-free and smooth surfaces of the films establish the potential of electrostatic spraying in synthesizing UHMWPE-GNP composite films at bulk-scale. Previous studies on low- and high-density polyethylene, reinforced with exfoliated graphite or GNPs, have employed melt mixing followed by twin-jet extrusion for fabricating composite pellets.^{9,10,34,35} The composite film fabrication through electrostatic spraying is an easy and rapid process for synthesis at macro-scale. Electrostatic spraying could be used directly for coating metallic implants in the intended application of UHMWPE-GNP composites. Easy flow of the composite powders through the nozzle of the spray gun aids in fabricating a coating with uniform thickness. The composite films were intentionally synthesized on nonstick Teflon coated surface for an easy peel-off without damaging them. Free standing films were required for assessing the mechanical properties through tensile testing.

3.2. Mechanical Properties of Films. Figure 3a presents the stress–strain curve obtained from the tensile tests of UHMWPE and UHMWPE-GNP composite films. Elastic modulus (*E*) is calculated from the slope of the initial straight line portion of each plot. Yield stress (YS) is defined at the point of the plot where it changes its slope for the first time.

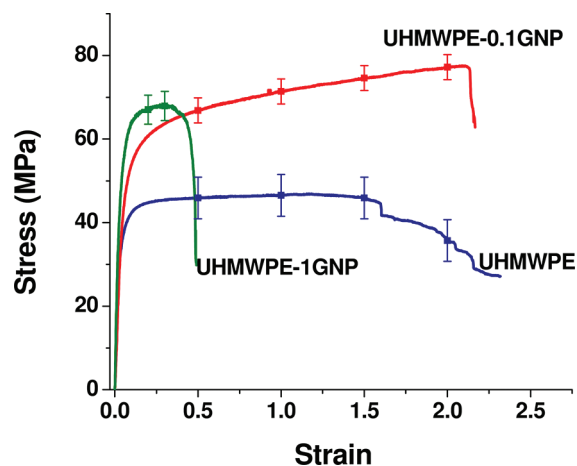


Figure 3. Stress strain plots of three films obtained from tensile tests.

Tensile strength (TS) is the highest stress the film could withstand. Area under each plot is computed to assess the fracture toughness in terms of amount of work per unit volume, which can be sustained by the films without failure. Table 1 presents the E , YS, TS, and work done per unit volume until failure point.

Table 1. Mechanical Properties of UHMWPE and UHMWPE-GNP Composite Films

sample	E (GPa)	YS (MPa)	TS (MPa)	work done until failure (J m^{-3})
PE	0.53 ± 0.03	22 ± 2.4	45 ± 4.9	$(98 \pm 10.8) \times 10^6$
PE-0.1GNP	0.69 ± 0.02	35 ± 1.4	77 ± 3.1	$(151 \pm 6.0) \times 10^6$
PE-1GNP	1.19 ± 0.08	42 ± 2.1	68 ± 3.4	$(30 \pm 1.5) \times 10^6$

Figure 3 and Table 1 reveal the improvement in mechanical properties of UHMWPE with addition of GNP. Elastic modulus of UHMWPE, UHMWPE-0.1GNP, and UHMWPE-1GNP is calculated to be 0.53, 0.69, and 1.19 GPa, which shows a gradual improvement of 27% and 124% with addition of 0.1 wt % and 1 wt % GNP respectively. Yield strength also follows similar trend with 59 and 90% improvement at 0.1 and 1 wt % GNP addition respectively. But, a maximum improvement in tensile strength (TS) up to 77 MPa is achieved at 0.1 wt % GNP content, as compared to 45 MPa in UHMWPE. Toughness also shows a peak in UHMWPE-0.1GNP, denoting 54% improvement over unreinforced polymer film. Both tensile strength and toughness deteriorates at 1 wt % GNP content. Figure 3a show very low fracture-strain of ~ 0.5 for UHMWPE-1GNP film, as compared to other two compositions having a similar fracture strain of ~ 2.2 . The low strain to failure for UHMWPE-1GNP has resulted in a significant 69% reduction in toughness as compared to UHMWPE film. An analysis of mechanical properties indicates differential strengthening mechanism governs deformation in elastic and plastic regime for UHMWPE-GNP composite system. E and YS show similar trend with GNP concentration, which is different from the trend shown by TS and toughness. This observation also indicates the strengthening mechanism is highly influenced by the microstructural changes in UHMWPE-GNP as a function of GNP content. The strengthening mechanism of UHMWPE-GNP system is discussed in the following section.

3.3. Strengthening Mechanism. Figure 4 presents the fracture surface of the UHMWPE-GNP films in three

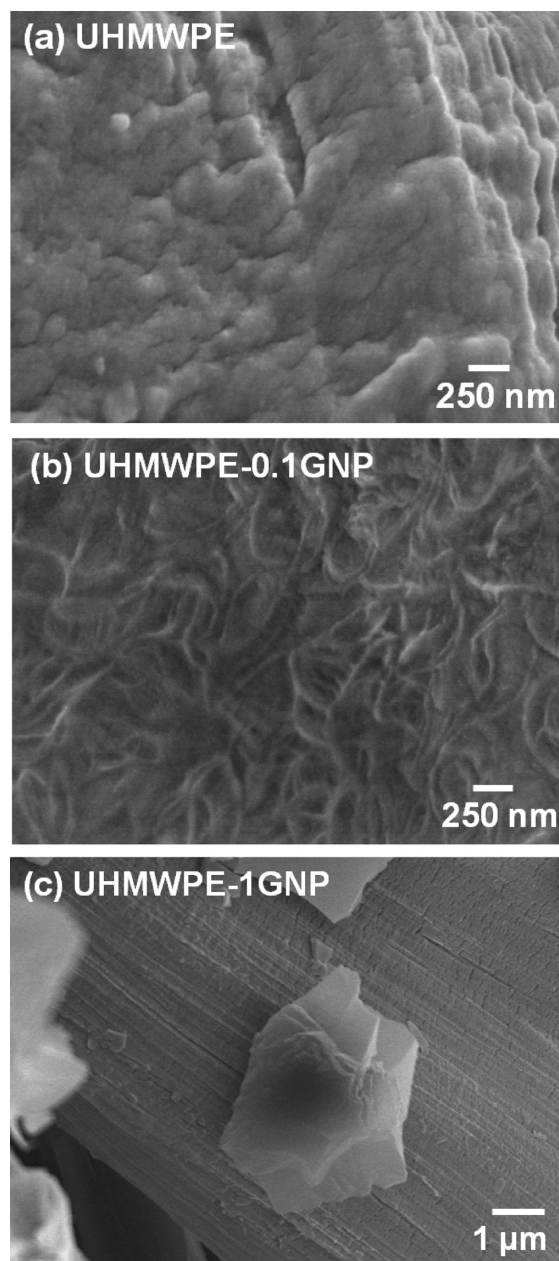


Figure 4. SEM images of fracture surfaces of (a) UHMWPE, (b) UHMWPE-0.1 GNP, and (c) UHMWPE-1GNP.

concentrations. Figure 4b shows uniform nanoscale wrinkles on the surface of UHMWPE-0.1GNP. Absence of similar feature on UHMWPE surface (Figure 4a) confirms the wrinkles being caused by the presence of GNP. The wrinkles originate from uniform wrapping of polymer on the inherent ripples of finely distributed graphene platelets. Similar features were also observed by Rafiee et al. on the fracture surface of epoxy-0.1 wt % graphene platelet composite.³ On the other hand, the fracture surface of UHMWPE-1GNP (Figure 4c) shows big clusters of GNPs loosely lying on the surface of the UHMWPE (Figure 4c). Agglomeration of GNPs at higher concentration causes big clusters, which could not be wrapped fully by polymer and thus do not get embedded in the matrix. This

observation is in full agreement with the distribution of GNP in UHMWPE-0.1GNP and UHMWPE-1GNP at the powder stage in Figure 1.

The distribution of GNP in UHMWPE has different strengthening effect in elastic and plastic regime. Due to random dispersion of GNPs, only a fraction will be oriented in such a way that their basal planes will be along the tensile axis. This fraction would absorb a significant amount of stress in the elastic regime, as the tensile load will be directly applied through in-plane direction of graphene and absorbed by covalent C–C bonds. In case of UHMWPE-1GNP, there is a probability of 10 times more GNPs oriented along tensile axis than in UHMWPE-0.1GNP, which can support more stress with low deformation. Thus a gradual increase in elastic modulus and yield strength is noted with increasing GNP concentration. It is emphasized that the increase in elastic modulus or yield strength from UHMWPE-0.1GNP to UHMWPE-1GNP is not 10 times largely because of the clustering of GNPs, which reduces its efficiency as reinforcement.³⁶

During the plastic deformation, the polymer–GNP interface strength becomes more critical, as effective load transfer between reinforcement and matrix is required to restrict deformation. In this regime, the GNPs oriented in directions other than tensile axis also take part in deformation, as the shear force becomes active along these interfaces to restrict the resulting elongation. Because of the presence of clustered GNPs in UHMWPE-1GNP, the shear force causes easy sliding between the graphene layers, which are bonded by weak van der Waal force. In addition, poor or no polymer wrapping on graphene (Figure 4c) causes ineffective load transfer leading to easy failure at weak polymer–graphene interface. Figure 5a shows separated and unembedded graphene layers from a graphene platelet on the fracture surface of UHMWPE-1GNP. The orientation of graphene layers clearly demark their easy sliding against one another, which does not support any load and thus has no effect on strengthening. Further evidence of ineffective GNP reinforcement is furnished in figure 5b, revealing unwrapped cluster of GNPs in the crack of fracture surface. Clustering of GNPs in UHMWPE-1GNP also causes nonuniform distribution of reinforcement phase in composite structure and more localized porosity. As a result, upon yielding, the composite fails in the weaker region of the structure, causing rapid failure at a very low strain and overall low toughness (figure 3a).

In the case of UHMWPE-0.1 GNP, the interface between polymer and GNP is strong because of better wrapping (Figure 4b). As a result, shear force is transferred effectively from the matrix to reinforcement.^{5,37} Moreover, due to excellent wrapping by polymer, the graphene layers cannot slide against each other and provides more strength. As observed in the stress–strain plot (Figure 3a) of UHMWPE-0.1GNP, the strength keeps on increasing with strain, thereby denoting strengthening. Because of better wrapping, the GNPs in almost any orientation become effective in UHMWPE-0.1GNP, causing higher strength than UHMWPE-1GNP. Ripples on graphene structure, along with uniform wrapping by polymer (Figure 4b), causes mechanical interlocking, leading to improved mechanical properties.^{3,4} Uniform distribution of GNP at low concentration (0.1 wt %) does not result in localized weak regions in the structure. Consequently, it can sustain more stress and strain without failure than other compositions. Figure 6 shows different evidence of GNP

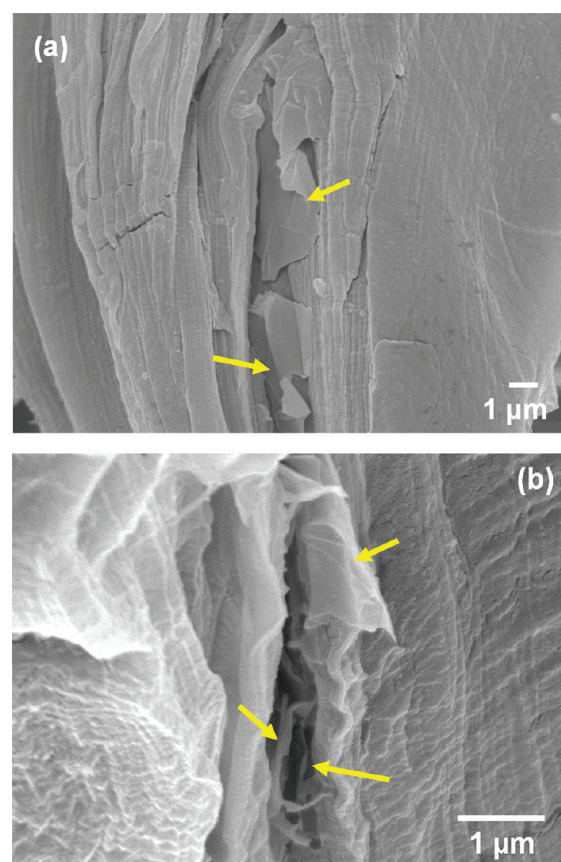


Figure 5. SEM micrograph on fracture surface of UHMWPE-1GNP revealing (a) easy sliding between graphene layers in unwrapped GNP; (b) presence of loose/unbonded GNP platelets in the cracks.

induced strengthening in UHMWPE-0.1GNP fracture surface. The protruded GNP on fracture surface with the base fully wrapped in polymer matrix (figure 6a) indicates the strength of polymer–GNP interface, which absorbs significant amount of energy before the final fracture. Figure 6b shows the presence of graphene on a fracture tip marked in the micrograph, which can be distinguished by its smoother surface compared to highly undulated surface of the surrounding polymer matrix. The presence of graphene at the fracture tip indicates that it supports and bears the stress until fracture. UHMWPE-0.1GNP shows similar total strain with UHMWPE, which denotes homogeneous dispersion-effect of reinforcement in the matrix. Thus the concentration of graphene is found very critical for strengthening of UHMWPE.

3.4. Biocompatibility of GNP and UHMWPE-GNP Composite. The cytotoxicity of GNP is assessed by incubating osteoblast in culture medium containing dispersed GNPs at different concentrations. Figure 7 presents the optical images of the cells incubated for a period of 5 days.

Morphological observations (Figure 7) suggest that all cells were attached but were considerably reduced in numbers with increasing graphene concentrations. This observation indicates negative effect of GNP on survival of bone forming cells. However, the effect on survival or shape of cells is least significant at the lowest concentration of 0.1 $\mu\text{g}/\text{mL}$. Literature has also reported the dose dependent cytotoxic effect of GNPs.^{27,28} Graphene concentration of 0.01–10 $\mu\text{g}/\text{mL}$ is reported to have no effect on death of PC12 neural cell lines.²⁸ In the present study, the cell shape and survival rate is found to

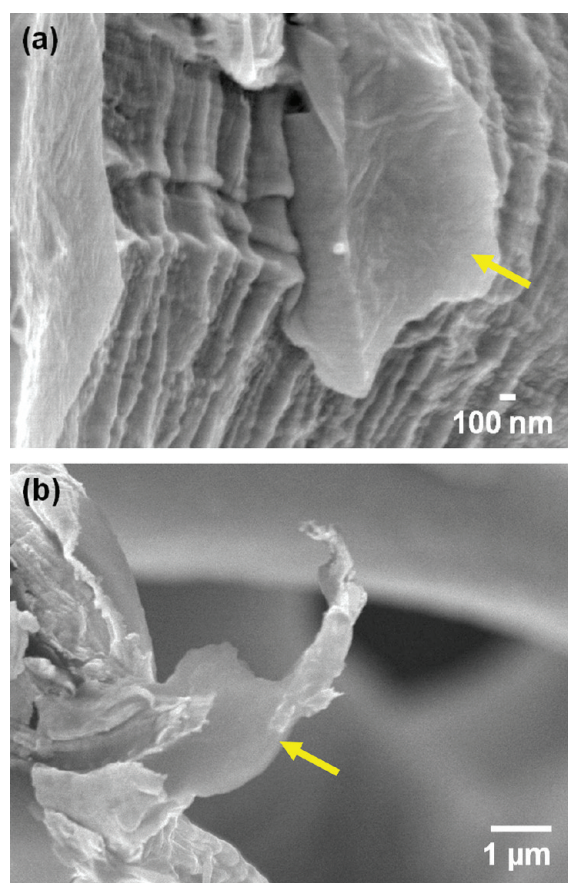


Figure 6. SEM micrograph on fracture surface of UHMWPE-0.1GNP revealing (a) protruded GNPs well-wrapped by polymer at base and (b) presence of GNP at the tip of fracture point.

be affected at $0.5 \mu\text{g/mL}$ and higher concentrations. The disparity with other published reports^{27,28} could be related to the cell type involved. Another important factor could be the agglomeration of GNPs to big clusters at higher concentrations in culture medium, which are observed as big black particles in Figure 7. The interaction of living cells with graphene is proposed to occur in three stages: (i) initial cell deposition on GNP, (ii) stress on the cell membrane due to contact with sharp edges of nanoplatelets and, (iii) inducing oxidative stress by generating reactive oxygen species.²⁷ The big clusters of GNPs at higher concentration can attach to cells easily on their surface and the sharp contact at cleavages and edges of graphene membranes could lead to membrane-rupture and cell death. Thus the reduction in osteoblast survival with GNP concentration could not only be related to the cytotoxicity of GNP, but is significantly influenced by its clustering.

Osteoblast cells were further incubated on electrostatically sprayed UHMWPE and UHMWPE-GNP composite films to evaluate the biocompatibility of these surfaces. The SRB assay results presented in Figure 8 indicates the survival rate of osteoblasts on the three films after different incubation periods.

Comparative reduction in the survival rate, presented in Table 2 helps in understanding the effect of GNP addition to the biocompatibility of UHMWPE films. Survival rate of osteoblasts is found decreasing with GNP content in UHMWPE (Figure 8). A reduction of osteoblast survivability by as much as 86.7% is observed after 5 days of incubation on UHMWPE-1GNP, in comparison to the control group (UHMWPE). In contrast, use of a small concentration of graphene (0.1 wt %) with the UHMWPE substrates permitted minimal cell necrosis, and ranged in the order of 6.6–16.6% reduction in viability in comparison to the controls (Figure 8). Observations reveal significantly decreased osteoblast survival

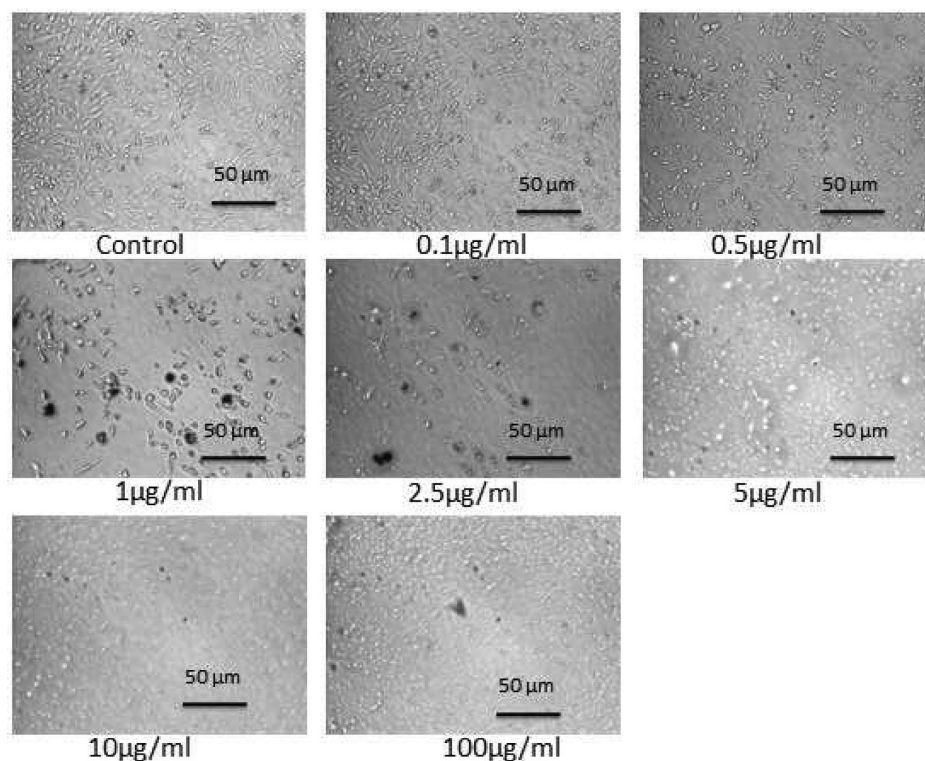


Figure 7. Optical images of osteoblast cells cultured for 5 days with different concentration of GNPs in culture medium.

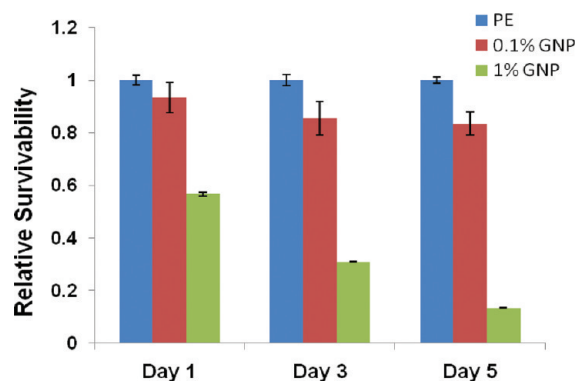


Figure 8. SRB test results of the three films showing the survival rate of osteoblasts cultured for different incubation periods.

Table 2. Percentage Reduction in Survivability of Osteoblasts between Different Substrates

incubation period (days)	compositions compared	reduction in survivability (%)
1	UHMWPE vs UHMWPE-0.1GNP	6.60
	UHMWPE vs UHMWPE-1GNP	43.33
	UHMWPE-0.1GNP vs UHMWPE-1GNP	36.73
3	UHMWPE vs UHMWPE-0.1GNP	14.43
	UHMWPE vs UHMWPE-1GNP	69.08
	UHMWPE-0.1GNP vs UHMWPE-1GNP	54.63
5	UHMWPE vs UHMWPE-0.1GNP	16.57
	UHMWPE vs UHMWPE-1GNP	86.66
	UHMWPE-0.1GNP vs UHMWPE-1GNP	70.09

rate in the UHMWPE-1GNP group with increasing number of days; however, it remains almost similar in UHMWPE-0.1GNP group for 3 and 5 days. Our observations are not in direct agreement with some of the reports available on response of osteogenic lineage to graphene or graphene reinforced composite surfaces. Mouse fibroblasts are found show normal proliferation and survival rate on graphene paper³³ and chitosan-graphene composite³¹ surfaces. Stem cells have also shown graphene induced accelerated growth toward osteogenic lineage.³⁰ Noncovalent binding abilities of graphene surface with osteogenic inducers are found to be responsible for stem cell growth and differentiation.³⁰ However, such preferential attachment of growth factors and favorable proteins are not possible on UHMWPE-0.1GNP surfaces, as the graphene surface is mostly wrapped by polymer. On the other hand, the UHMWPE-1GNP might have some exposed surfaces of GNP clusters, but their sharp edges might be detrimental to osteoblast viability as discussed above, which causes the gradual decrease in osteoblast survivability on this surface.

A 6–16% decrease in osteoblast survivability for UHMWPE-0.1GNP could also be attributed to the absorption of cell culture medium in the composite film, followed by traces of GNP leaching into the medium that causes necrosis of osteoblasts. Other researchers have also reported absorption of water and bovine serum on UHMWPE surface deteriorating its wear resistance.³⁸ Because most of the GNPs in UHMWPE-

0.1GNP film are wrapped with polymer (Figure 4b), only traces of unwrapped GNPs may be available for leaching. It is expected that most of the unwrapped GNPs will go into the solution during an initial exposure period. As a result, the reduction in survivability of osteoblasts is up to 14% in the first 3 days, but is relatively unchanged at 5 days. On the other hand, clusters and unwrapped GNPs in UHMWPE-1GNP film support a continuous leaching of GNPs with time and leads to increasing osteoblast death rate (86.7%) up to 5 days.

In light of the discussion on mechanical properties and biocompatibility, we found PE-0.1GNP shows excellent improvement in mechanical properties, with slightly reduced biocompatibility as compared to UHMWPE. However, the biocompatibility of UHMWPE-GNP composite has shown a clear trend of relative improvement with lower GNP concentration. In this scenario, a composition of GNP could be further optimized by extending to levels below 0.1 wt %, thereby permitting a satisfactory improvement in mechanical properties without sacrificing the biocompatibility.

4. CONCLUSION

Electrostatic spraying is established as a rapid fabrication method for freestanding UHMWPE-GNP composite coatings at bulk-scale. The concentration of GNP is found critical for improvement in mechanical properties. Fracture toughness of UHMWPE increases from 98×10^6 J/m³ to 151×10^6 J/m³ at UHMWPE-0.1GNP, but decreases to 30×10^6 J/m³ in UHMWPE-1GNP. Similar trend is observed for tensile strength also with a maximum of 71% improvement at 0.1 wt.% GNP loading. On the contrary, elastic modulus and yield strength shows an increasing trend with GNP content, with an impressive 124% and 90% improvement, respectively, in UHMWPE-1GNP. Graphene content along with its distribution and matrix-reinforcement interfacial bonding are found activating the differential strengthening mechanism in elastic and plastic deformation regime. The biocompatibility of GNP and UHMWPE-GNP composite to osteoblast cells are found to be dose-dependent. The cytotoxicity of GNP in the present study is also influenced by agglomeration of GNPs. UHMWPE-GNP composite shows better biocompatibility at low GNP concentration. This study suggests GNP content lower than 0.1 wt % may promote further optimization with significant improvement in mechanical properties and required biocompatibility for orthopedic applications.

AUTHOR INFORMATION

Corresponding Author

*E-mail: e-mail:agarwala@fiu.edu. Phone: (305) 348-1701. Fax: 1-305-348-1932.

Notes

The authors declare no competing financial interest.

ACKNOWLEDGMENTS

A.A. acknowledges support from National Science Foundation CAREER Award (NSF-DMI-0547178) and US Air Force Office of Scientific Research (FA9550-09-1-0297). SR and RD acknowledge support through a RESEED award, from the College of Engineering and Computing, Florida International University. The overall support of Mr. Neal Ricks and AMERI at FIU, in providing the research facilities is greatly acknowledged. I.N. (Christopher Columbus High School, Miami) and A.B. (John A. Ferguson Senior High School, Miami) are high

school students who performed research as summer interns and would like to acknowledge their respective schools, for encouragement in scientific/research activities.

■ REFERENCES

- (1) Soldano, C.; Mahmood, A.; Dujardin, E. *Carbon* **2010**, *48*, 2127–2150.
- (2) Kuilla, T.; Bhadra, S.; Yao, D.; Kim, N. H.; Bose, S.; Lee, J. H. *Prog. Polym. Sci.* **2010**, *35*, 1350–1375.
- (3) Rafiee, M. A.; Rafiee, J.; Wang, Z.; Song, H.; Yu, Z.-Z.; Koratkar, N. *ACS Nano* **2009**, *3*, 3884–3890.
- (4) Das, B.; Prasad, K. E.; Ramamurty, U.; Rao, C. N. R. *Nanotechnology* **2009**, *20*, 125705.
- (5) Fang, M.; Wang, K.; Lu, H.; Yang, Y.; Nutt, S. J. *Mater. Chem.* **2009**, *19*, 7098–7105.
- (6) Ji, X.-Y.; Cao, Y.-P.; Feng, X.-Q. *Modell. Simul. Mater. Sci. Eng.* **2010**, *18*, 045005.
- (7) Rafiee, M. A.; Rafiee, J.; Srivastava, I.; Wang, Z.; Song, H.; Yu, Z.-Z.; Koratkar, N. *Small* **2010**, *6*, 179–183.
- (8) Kim, H.; Abdala, A. A.; Makosko, C. W. *Macromolecules* **2010**, *43*, 6515–6530.
- (9) Kim, S.; Do, I.; Drazl, L. T. *Polym. Compos.* **2010**, *31*, 755–761.
- (10) Zheng, W.; Lu, X.; Wong, S.-C. *J. Appl. Polym. Sci.* **2004**, *91*, 2781–2788.
- (11) Stankovich, S.; Dikin, D. A.; Dommett, G. H. B.; Kohlhaas, K. M.; Zimney, E. J.; Stach, E. A.; Piner, R. D.; Nguyen, S. T.; Ruoff, R. S. *Nature* **2006**, *442*, 282–286.
- (12) Eda, G.; Unalan, H. E.; Rupasinghe, N.; Amaratunga, G. A. J.; Chhowalla, M. *Appl. Phys. Lett.* **2008**, *93*, 233502.
- (13) Ramanathan, T.; Abdala, A. A.; Stankovich, S.; Dikin, D. A.; Herrera-Alonso, M.; Piner, R. D.; Adamson, D. H.; Schniepp, H. C.; Chen, X.; Ruoff, R. S.; Nguyen, S. T.; Aksay, I. A.; Prud'Homme, R. K.; Brinson, L. C. *Nat. Nanotechnol.* **2008**, *3*, 327–331.
- (14) Tang, H.; Ehlert, G. J.; Lin, Y.; Sodano, H. A. *Nano Lett.* **2012**, *12*, 84–90.
- (15) Wei, T.; Luo, G.; Fan, Z.; Zheng, C.; Yan, J.; Yao, C.; Li, W.; Zhang, C. *Carbon* **2009**, *47*, 2290–2299.
- (16) Vadukumpally, S.; Paul, J.; Mahanta, N.; Valiyaveetil, S. *Carbon* **2011**, *49*, 198–205.
- (17) Cao, Y.; Feng, J.; Wu, P. *Carbon* **2010**, *48*, 3834–3839.
- (18) Branch del Prever, E. M.; Bistolfi, A.; Bracco, P.; Costa, L. J. *Orthopaed. Traumatol.* **2009**, *10*, 1–8.
- (19) Ingham, E.; Fisher, J. *Biomaterials* **2005**, *26*, 1271–1286.
- (20) Fang, L.; Gao, P.; Leng, Y. *Composite B* **2007**, *38*, 345–351.
- (21) Fang, L.; Leng, Y.; Gao, P. *Biomaterials* **2006**, *27*, 3701–3707.
- (22) Xue, Y.; Wu, W.; Jacobs, O.; Schadel, B. *Polym. Testing* **2006**, *25*, 221–229.
- (23) Ruan, S.; Gao, P.; Yu, T. X. *Polymer* **2006**, *47*, 1604–1611.
- (24) Ruan, S. L.; Gao, P.; Yang, X. G.; Yu, T. X. *Polymer* **2003**, *44*, 5643–5654.
- (25) Bakshi, S. R.; Tercero, J. E.; Agarwal, A. *Composites A* **2007**, *38*, 2493–2499.
- (26) Delgado, A.; Addiego, F.; Ahzi, S.; Patlazhan, S.; Toniazzo, V.; Ruch, D. *IOP Conf. Ser.: Mater. Sci. Eng.* **2012**, *31*, 012009.
- (27) Liu, S.; Zeng, T. H.; Hofmann, M.; Burcombe, E.; Wei, J.; Jiang, R.; Kong, J.; Chen, Y. *ACS Nano* **2011**, *5*, 6971–6980.
- (28) Zhang, Y.; Ali, S. F.; Dervishi, E.; Xu, Y.; Li, Z.; Casciano, D.; Biris, A. S. *ACS Nano* **2010**, *4*, 3181–3186.
- (29) Wang, K.; Ruan, J.; Song, H.; Zhang, J.; Wo, Y.; Guo, S.; Cui, D. *Nanoscale Res. Lett.* **2011**, *6*, 1–8.
- (30) Lee, W. C.; Lim, C. H. Y. X.; Shi, H.; Tang, L. A. L.; Wang, Y.; Lim, C. T.; Loh, K. P. *ACS Nano* **2011**, *5*, 7334–7341.
- (31) Fan, H.; Wang, L.; Zhao, K.; Li, N.; Shi, Z.; Ge, Z.; Jin, Z. *Biomacromolecules* **2010**, *11*, 2345–2351.
- (32) Kim, S.; Ku, S. H.; Lim, S. Y.; Kim, J. H.; Park, C. B. *Adv. Mater.* **2011**, *23*, 2009–2014.
- (33) Chen, H.; Muller, M. B.; Gilmore, K. J.; Wallace, G. G.; Li, D. *Adv. Mater.* **2008**, *20*, 3557–3561.
- (34) Kim, S.; Seo, J.; Drzal, L. T. *Composites A* **2010**, *41*, 581–587.
- (35) Kim, S.; Do, I.; Drazl, L. T. *Macromol. Mater. Eng.* **2009**, *294*, 196–205.
- (36) Shi, D. -L.; Feng, X. -Q.; Huang, Y. Y.; Hwang, K. -C.; Gao, H. *Trans. ASME* **2004**, *126*, 250–257.
- (37) Gong, L.; Kinloch, I. A.; Young, R. J.; Riaz, I.; Jalil, R.; Novoselov, K. S. *Adv. Mater.* **2010**, *22*, 2694–2697.
- (38) Lاراia, K.; Leone, N.; MacDonald, R.; Blanchet, T. A. *Tribol. Trans.* **2006**, *49*, 338–346.